

Angewandte

International Edition

Www.angewandte.org

Hydrogen-Bonded Organic Frameworks

How to cite: Angew. Chem. Int. Ed. **2025**, 64, e202507332 doi.org/10.1002/anie.202507332

# $\pi$ - $\pi$ Stacking as Electron-Transfer Channels in Hydrogen-Bonded Organic Frameworks for Boosting Photocatalysis

Jian-Hua Mei<sup>+</sup>, Ya-Ru Zeng<sup>+</sup>, Yun-Nan Gong, Wen-Jie Shi, Di-Chang Zhong,\* and Tong-Bu Lu

**Abstract:** Photocatalysis provides a promising approach to produce green energy, by which the intermittent solar energy can be converted into storable chemical energy. It is well-known that the electron-transfer rate has great influence on the photocatalytic efficiency. Revealing the influence of electron-transfer rate on the photocatalytic efficiency from a molecular level is of great significance but a challenge. Herein, we give solid evidence to show that the  $\pi$ - $\pi$  stacking can serve as an electrontransfer channel to boost photocatalysis. Specifically, two hydrogen-bonded organic frameworks (HOFs) with similar structures but slightly different intermolecular interactions have been weaved. Interestingly, the HOF with  $\pi$ - $\pi$  stacking interactions shows much higher photocatalytic activity for hydrogen evolution than the one without. Further structural and spectroscopic analyses revealed that the much-enhanced photocatalytic activity of the former can be attributed to the  $\pi$ - $\pi$  stacking, which can really serve as an electron-transfer channel, thus accelerating the electron transfer and achieving a remarkably enhanced activity in photocatalytic hydrogen evolution. The work, from a molecular level, reveals the role of  $\pi$ - $\pi$  stacking in photocatalysis and gives new insights into the electron-transfer in photocatalysts.

#### Introduction

Solar energy-driven water splitting and/or CO<sub>2</sub> reduction is considered a promising strategy to convert and store the intermittent solar energy.<sup>[1–30]</sup> However, the currently low photocatalytic conversion efficiency limits the industrial application of this technology. It is well-known that accelerating the electron transfer in photocatalysts is beneficial for enhancing the photocatalytic efficiency. In this aspect,

[\*] J.-H. Mei<sup>+</sup>, Y.-R. Zeng<sup>+</sup>, Dr. Y.-N. Gong, Dr. W.-J. Shi, Prof. Dr. D.-C. Zhong, Prof.Dr. T.-B. Lu Institute for New Energy Materials and Low Carbon Technologies, School of Materials Science and Engineering, Tianjin University of Technology, Tianjin 300384, China E-mail: dczhong@email.tjut.edu.cn

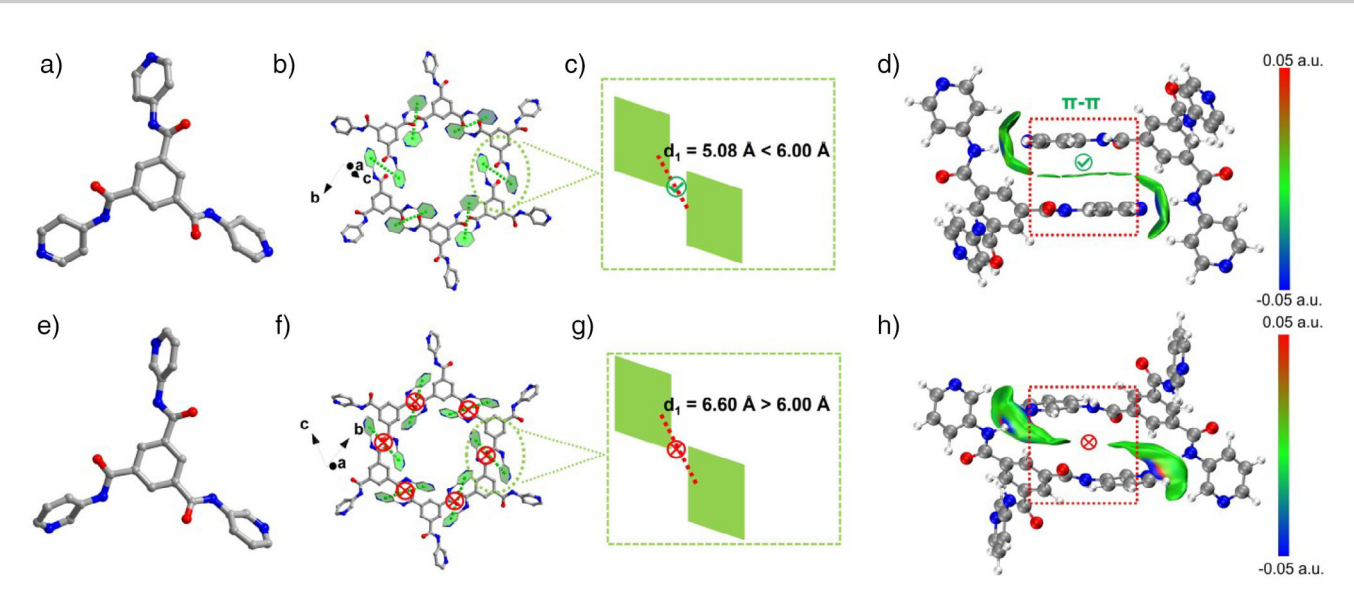
diverse strategies have been developed recently to expedite electron transfer and achieve remarkable photocatalytic efficiency. [6-14] For instance, the introduction of an additional redox mediator as an electron relay can accelerate the electron transfer from the excited photosensitizer to catalyst, resulting in much enhanced photocatalytic efficiency.[11-14] In addition, the covalent connection of photosensitizer and catalyst can also achieve ultrafast electron transfer.[15-21] As a representative example, Nakada et al. have coupled Re/Mn catalyst and Ru/Os photosensitizer via covalent bonds to facilitate the intermolecular electron delivery and thus enhance photocatalytic activity.[15-19] Ouyang group designed an Ir(III) photosensitizer featuring a pyridine-type ligand to connect molecular catalysts, which also achieved improved photocatalytic efficiency.<sup>[21]</sup> In heterogeneous systems, grafting molecular catalysts onto organic semiconductors such as g-C<sub>3</sub>N<sub>4</sub> has also achieved rapid charge transfer and high activity in photocatalysis.[22-25]

In addition to the traditional covalent strategy, noncovalent interactions can also facilitate the electron transfer to boost photocatalysis, which has been demonstrated in homogeneous photocatalytic systems.<sup>[26–30]</sup> Kubiak group has found that the hydrogen-bonding interactions between a Re bipyridine catalyst and a Ru photosensitizer contribute to the intermolecular electron transfer, thus greatly enhancing the photocatalytic activity for CO<sub>2</sub> reduction.<sup>[26]</sup> Ouyang and coworkers have reported that a Cu(I) photosensitizer and a pyrene-appended Co(II) catalyst can be preassembled by  $\pi$ - $\pi$  stacking interactions, which expedites the intermolecular electron transfer and thus boosts the CO<sub>2</sub> photoreduction.<sup>[27]</sup> Despite the non-covalent interactions being reasoned for the activity enhancement in these homogeneous photocatalytic systems, such non-covalent interactions were determined by spectroscopic analyses.<sup>[27–30]</sup> The contribution of non-covalent interactions in accelerating electron transfer and boosting catalytic activity has not been directly observed.

Hydrogen-bonded organic frameworks (HOFs) are a new class of porous crystalline materials. [31–35] Owing to well-defined and tailorable structures, semiconductor-like behavior, and self-healing ability, HOFs have currently shown potential application in photocatalysis. [36–41] These features of HOFs also provide a good platform for studying the effect of non-covalent interactions on accelerating electron transfer and boosting photocatalytic activity. In this article, we demonstrate that  $\pi$ - $\pi$  stacking can serve as an electron-transfer channel to boost photocatalysis, based on the fact that two HOFs with similar structures but slightly different

<sup>[+]</sup> Both authors contributed equally to this work.

Additional supporting information can be found online in the Supporting Information section



**Scheme 1.** Schematic of the  $\pi$ - $\pi$  stacking modes in HOF-8 a-d) and HOF-TUT-8 e-h) (the color of the bar in d and h, red: prominent repulsive interaction; green: van der Waals interaction; blue: prominent attractive weak interaction).

intermolecular interactions as well as big different photocatalytic activity in hydrogen evolution. Specifically, HOF-8, a reported HOF based on N1, N3, N5-tri(pyridin-4-yl)benzene-1,3,5-tricarboxamide (L<sub>1</sub>; Scheme 1a), [42] and HOF-TUT-8, a new HOF based on N<sup>1</sup>, N<sup>3</sup>, N<sup>5</sup>-tri(pyridin-3-yl)benzene-1,3,5-tricarboxamide (L2; Scheme 1e) have been assembled, in which the only difference between them is the  $\pi$ - $\pi$  stacking interactions (Scheme 1b-d,f-h). Interestingly, HOF-8 with  $\pi$ - $\pi$  stacking interactions exhibits outstanding photocatalytic activity for water splitting, with H<sub>2</sub> evolution rate of 3.3 times higher than that of HOF-TUT-8 with negligible  $\pi$ - $\pi$  stacking interactions, highlighting the  $\pi$ - $\pi$  stacking interactions in boosting photocatalysis. The combined results of linear sweep voltammetry (LSV) and time-resolved fluorescence spectroscopic measurements reveal that the electron transfer in HOF-8 is really faster than that in HOF-TUT-8, well supporting the higher photocatalytic activity of HOF-8 for H<sub>2</sub> evolution. This study for the first time structurally shows  $\pi - \pi$ stacking interactions as electron-transfer channels in boosting photocatalysis.

#### **Results and Discussion**

 $L_1$  and  $L_2$  were synthesized by modified condensation amidation reactions, respectively (see the Supporting Information). The nuclear magnetic resonance hydrogen spectra ( $^1H$  NMR) and Fourier transform infrared spectroscopy (FTIR) spectra of  $L_1$  and  $L_2$  revealed that they were successfully synthesized with high purity (Figures S1–S3). Recrystallization of  $L_1$  and  $L_2$  in the mixed solvent of CHCl<sub>3</sub>/CH<sub>3</sub>OH (3:1,  $\nu/\nu$ ) and CHCl<sub>3</sub>/CH<sub>3</sub>CN/CH<sub>3</sub>OH (6:1:1,  $\nu/\nu/\nu$ ), respectively, affords single crystals of HOF-8[ $^{42}$ ] and HOF-TUT-8, respectively (see the Supporting Information). The scanning electron microscopy (SEM) images show that the morphologies of

both HOF-8 and HOF-TUT-8 are block-shaped with similar sizes (Figure S4).

Single-crystal X-ray diffraction analysis reveals that HOF-8 and HOF-TUT-8 crystallize in the monoclinic space group of  $C2/c^{42}$  and the triclinic space group of  $P-1P\overline{1}$ , respectively (Table S1). As shown in Figure 1a,b, each L1 in HOF-8 connects with three other L<sub>1</sub> through three pairs of hydrogen bonds (N1-H1...N6, N3-H3...N2, and N5-H5•••N4), generating a two-dimensional (2D) layer structure (Table S2). [42,44–49] Adjacent layers are stacked through  $\pi$ – $\pi$ stacking interactions to form a three-dimensional (3D) porous framework with the pore size of  $6.8 \times 4.5 \text{ Å}$  (Figure 1c,d and Figure S5; Tables S3 and S4). Similar to HOF-8, each L<sub>2</sub> in HOF-TUT-8 also links three adjacent L<sub>2</sub> by three pairs of hydrogen bonds (N1-H1•••N6, N3-H3•••N2, and N5-H5•••N4) to form a 2D layer structure (Figure 1e,f). The adjacent 2D layers in HOF-TUT-8 are further connected through hydrogen bonds (C10-H10•••O2, C16-H16•••O3, C22-H22•••O1, and C24-H24•••O3) to generate a 3D porous framework (Figure 1h and Figure S6), rather than  $\pi - \pi$ stacking interactions as in HOF-8 because of the long distances and large dihedral angles between the pyridine rings (Tables \$5 and \$6). The pore size of HOF-TUT-8 is approximately  $6.2 \times 4.2$  Å, which is similar to that of HOF-8 (Figure 1f-h). Energy decomposition analysis was further carried out to quantitatively calculate the intermolecular interactions between L<sub>1</sub> monomers in HOF-8, and L<sub>2</sub> monomers in HOF-TUT-8 (see the Supporting Information). The results show that dispersion force dominates the total interactions in HOF-8, with the energy of  $-101.80 \text{ kJ mol}^{-1}$ , higher than that in HOF-TUT-8 (Scheme 1d,h, Table S7). This result further illustrates the stronger supramolecular interactions in HOF-8 over HOF-TUT-8.

Powder X-ray diffraction (XRD) patterns show that the measured patterns of HOF-8 and HOF-TUT-8 closely match those of the simulated ones generated from their single crystal data, indicative of their high purity (Figure 2a). The FT-IR

18213773, 2025, 29, Downloaded from https://onlinelibrary.wiley.com/doi/10.1002/anie.202507332 by Tianjin University Of, Wiley Online Library on [06/10/2025]. See the Terms and Conditions (https://onlinelibrary.wiley.com/erms-and-conditions) on Wiley Online Library for rules of use; OA articles are governed by the applicable Creative Commons Licenses

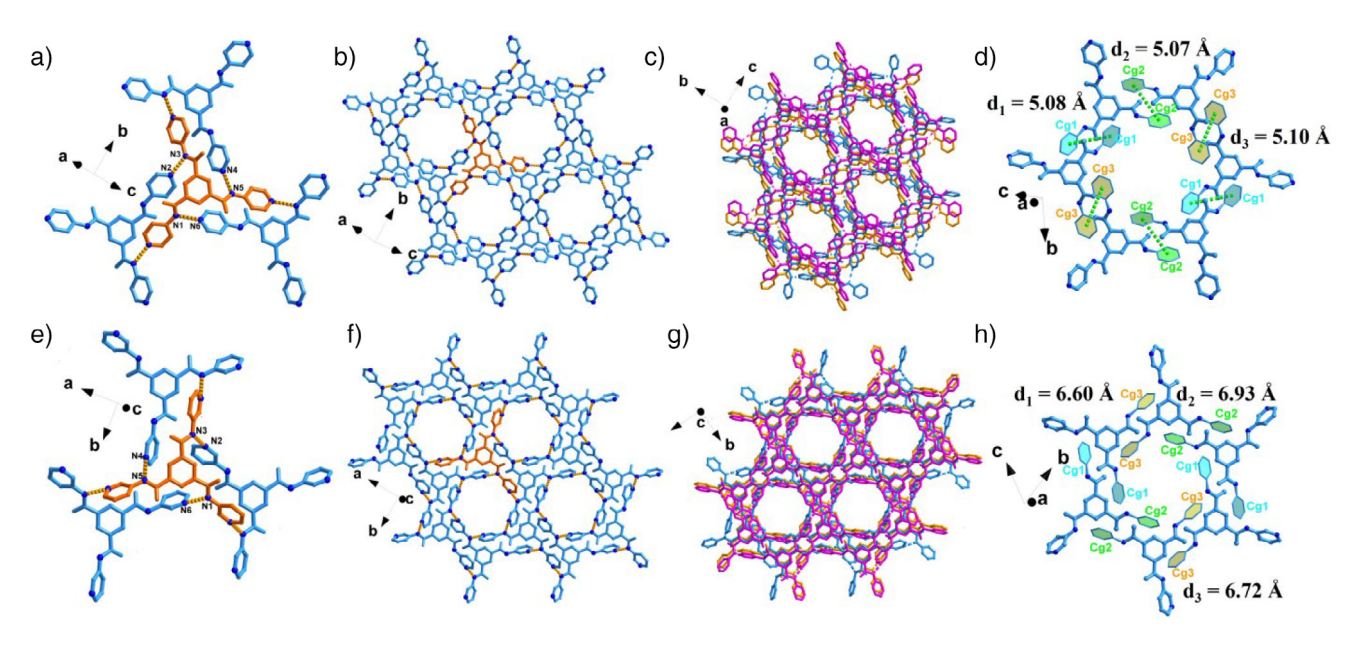


**Figure 1.** a) Hydrogen bonds in HOF-8. b) 2D supramolecular layer of HOF-8. c) 3D supramolecular microporous structure of HOF-8. d)  $\pi-\pi$  stacking interactions in HOF-8 (d:  $C_g \cdots C_g$  distance). e) Hydrogen bonds in HOF-TUT-8. f) 2D supramolecular layer of HOF-TUT-8. g) 3D supramolecular microporous structure of HOF-TUT-8. h) The negligible  $\pi-\pi$  stacking interactions in HOF-TUT-8 (d:  $C_g \cdots C_g$  distance).

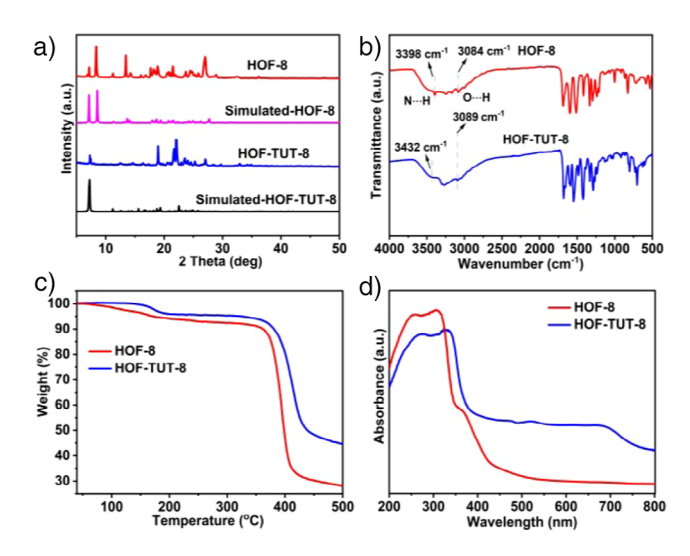


*Figure 2.* a) Powder XRD patterns, b) FTIR spectra, c) TG curves, and d) solid UV–vis spectra of HOF-8 (a new sample of HOF-8 was synthesized, and these data were obtained by repeated measurements) and HOF-TUT-8.

spectra of HOF-8 and HOF-TUT-8 display N–H stretching vibration peaks at 3398 and 3432 cm<sup>-1</sup> respectively, corresponding to N–H···N hydrogen bonds (Figure 2b). [44–49] These results agree with their crystal structures (Tables S2–S6). X-ray photoelectron spectroscopic (XPS) measurements were performed to identify the chemical compositions of HOF-8 and HOF-TUT-8 (Figures S7–S9). The XPS spectra show the C 1 s spectra display characteristic peaks at approximately 284 and 288 eV, corresponding to C–C/C=C and N–C=O, respectively. For O 1 s, two characteristic peaks at approximately 531 and 533 eV were observed, which can be assigned

to C=O and C-O, respectively. For N 1 s, two characteristic peaks at approximately 399 and 400 eV appeared, corresponding to pyridine N and N-C=O, respectively.<sup>[37,44,50-53]</sup> Thermogravimetric analysis (TGA) revealed that the two HOFs exhibit good thermal stability, with the decomposition temperature over 350 °C (Figure 2c).

The porous features of HOF-8 and HOF-TUT-8 were evaluated by CO<sub>2</sub> sorption tests at 196 K and 1 atm. As shown in Figures S10 and S11, HOF-8 and HOF-TUT-8 exhibit similar CO<sub>2</sub> adsorption capacity at 196 K with adsorption amounts of 24.99 and 24.09 cm<sup>3</sup> g<sup>-1</sup>, respectively. The corresponding Brunauer-Emmett-Teller (BET) surface areas are 109.46 and 90.88  $m^2$   $g^{-1}$ , respectively.<sup>[37,41,54–57]</sup> To further examine their porosity, the I<sub>2</sub> adsorption experiments were conducted by soaking HOF-8 and HOF-TUT-8 in nhexane solution of I<sub>2</sub> (Figures S12 and S13). The adsorption of HOF-8 and HOF-TUT-8 to I2 was clearly observed by the color change of the solution from pink to colorless after 8 and 12 h, respectively. Moreover, the UV-vis spectra show that the intensity of I<sub>2</sub> characteristic peak at about 521 nm gradually decreases with increasing soaking time, further confirming the presence of porosity in HOF-8 and HOF-TUT-8 (Figures S12 and \$13).

The results of solid UV-vis spectra demonstrate that HOF-8 and HOF-TUT-8 exhibit main light absorption in the UV region and weak light absorption in visible region (Figure 2d). The band gap energies ( $E_{\rm g}$ ) of HOF-8 and HOF-TUT-8 are determined based on their solid UV-vis spectra, which are 3.48 and 3.33 eV, respectively (Figures S14 and S15). In addition, the lowest unoccupied molecular orbital (LUMO) levels of HOF-8 and HOF-TUT-8 are estimated as -0.98 and -1.02 V versus NHE, respectively, by Mott-Schottky measurements (Figure S16). Hence, their highest occupied molecular orbitals (HOMOs) could be calculated

15213773, 2025, 29, Downloaded from https://onlinelibrary.wiley.com/oi/10.1002/anie.202507332 by Tanjan University Of, Wiley Online Library on 106/10/2025, See the Terms and Conditions (https://onlinelibrary.wiley.com/terms-and-conditions) on Wiley Online Library for rules of use; OA articles are governed by the applicable Creative Commons License

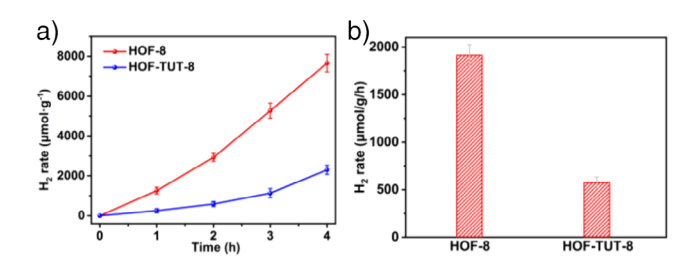


**Figure 3.** a) Kinetic profiles of photocatalytic  $H_2$  evolution over HOF-8 and HOF-TUT-8. b) Comparison of the photocatalytic activity of HOF-8 and HOF-TUT-8 for  $H_2$  evolution. The error bars are standard deviations calculated from the results of three repeated experiments.

to be 2.50 and 2.31 V versus NHE, respectively. Notably, the LUMO positions of HOF-8 and HOF-TUT-8 are lower than the proton reduction needed (-0.42 V vs. NHE, pH 7), suggesting that they are thermodynamically capable of photocatalytic proton reduction (Figure S17).<sup>[58,59]</sup>

On the basis of the above results, photocatalytic hydrogen evolution experiments of HOF-8 and HOF-TUT-8 were conducted in aqueous solution under UV–visible light irradiation ( $\lambda \geq 320$  nm), with 51 µL 0.014 M K<sub>2</sub>PtCl<sub>4</sub> aqueous solution and triethylamine (TEA) as the sacrificial agent (see the Supporting Information). Interestingly, despite the packing modes of HOF-8 and HOF-TUT-8 are almost the same, HOF-8 exhibits a much higher hydrogen production rate of 1914.4 µmol g<sup>-1</sup> h<sup>-1</sup>, which is over three times of HOF-TUT-8 (Figure 3 and Table S8, entries 1–2). Moreover, the H<sub>2</sub> production rate of HOF-8 is also superior to most of the reported photocatalysts under similar reaction conditions (Table S9).

A series of control experiments of photocatalytic H<sub>2</sub> evolution with HOF-8 revealed that negligible or even no H<sub>2</sub> was detected in the absence of HOF-8, TEA, or light irradiation (Table \$8, entries 3-5), indicating that HOF-8, TEA and light are all indispensable to the photocatalytic H<sub>2</sub> evolution. The photocatalytic durability of HOF-8 was evaluated via recycling experiments. No obvious decrease in the H<sub>2</sub> evolution process was observed during the four consecutive cycles (Figure \$18). SEM images reveal that the morphologies of HOF-8 and HOF-TUT-8 after photocatalytic reaction change to microcrystals, which are similar to those freshly prepared (Figure S19). Furthermore, the powder XRD patterns reveal almost unchanged crystallinity and structural integrity of HOF-8 and HOF-TUT-8 after photocatalytic H<sub>2</sub> evolution reaction (Figures \$20 and \$21), and the UV-vis spectra show almost no organic monomers were leached during the photocatalytic process (Figures S22 and S23). In addition, the FT-IR spectra of HOF-8 and HOF-TUT-8 before and after the photocatalytic reactions are also similar (Figures S24 and S25). These results demonstrate the excellent stability of HOF-8 and HOF-TUT-8 during the photocatalytic H<sub>2</sub> evolution processes.

To elucidate the better photocatalytic activity of HOF-8 over HOF-TUT-8 for H<sub>2</sub> evolution, photocurrent, electrochemical impedance spectroscopy (EIS), photoluminescence (PL), and time-resolved PL (TRPL) measurements were performed.<sup>[60-64]</sup> As shown in Figure 4a, HOF-8 exhibited a

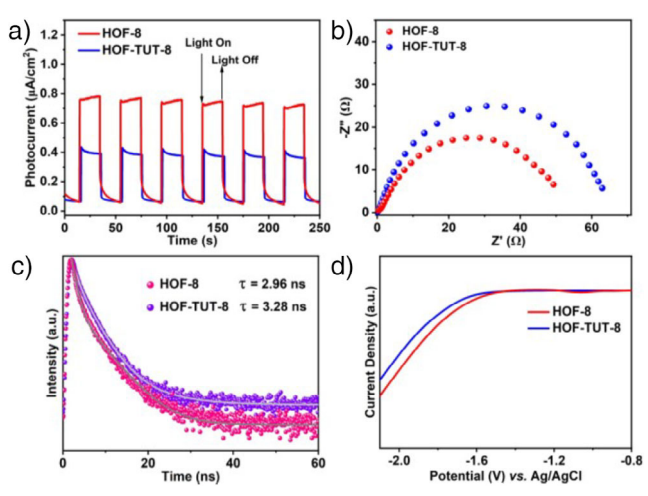


**Figure 4.** a) Photocurrent tests, b) EIS plots, c) time-resolved fluorescence spectroscopy ( $\lambda_{ex}=365$  nm and  $\lambda_{em}=420$  nm), and d) linear sweep voltammetry (LSV) curves for HOF-8 and HOF-TUT-8.

higher photocurrent response than HOF-TUT-8, indicating that HOF-8 has a faster electron transfer-rate. EIS results demonstrated that compared with HOF-TUT-8, HOF-8 showed a smaller semicircle radius, indicating lower charge-transfer resistance of HOF-8 (Figure 4b).

Moreover, the PL and TRPL spectra displayed that the emission intensity and PL lifetime of HOF-8 were weaker and shorter, respectively, than those of HOF-TUT-8, suggesting more efficient charge separation and transfer for HOF-8 than for HOF-TUT-8 (Figure \$26, Figure 4c, and Table \$10). Besides, the linear sweep voltammetry (LSV) measurements of HOF-8 and HOF-TUT-8 were conducted in Ar atmosphere to study the thermodynamics of H<sub>2</sub> evolution. As shown in Figure 4d, HOF-8 exhibited lower onset overpotential and higher current density than HOF-TUT-8, implying that HOF-8 is thermodynamically superior to HOF-TUT-8. Moreover, the terephthalic acid photoluminescence probing technique (TA-PL) of HOF-8 and HOF-TUT-8 was used to investigate the formation of •OH species. As shown in Figure \$27, both HOF-8 and HOF-TUT-8 display PL signals, indicative of 'OH species formation. HOF-8 shows stronger signal than HOF-TUT-8, demonstrating that HOF-8 possesses more photogenerated electrons, which suggests better charge separation efficiency. [62,65,66] The above results clearly demonstrated that HOF-8 exhibited more efficient charge separation and transfer than HOF-TUT-8, thus accounting for the higher photocatalytic activity for H<sub>2</sub> evolution.

The possible mechanism for photocatalytic  $H_2$  evolution over HOF-8 or HOF-TUT-8 was elucidated by in situ electron paramagnetic resonance (EPR) and XPS measurements. The results of EPR demonstrated that both HOF-8 and HOF-TUT-8 exhibited stronger signals at g=2.00 under light compared with those in the dark, implying that some holes were produced upon light illumination (Figures S28 and S29). [67,68] In this case, the photogenerated electrons can easily transfer to the Pt cocatalyst to reduce  $H^+$  to  $H_2$ . Furthermore, the N 1 s XPS spectrum of Pt/HOF-8 displays two characteristic peaks at 398.8 and 400.1 eV in the dark,

15213773, 2025, 29, Downloaded from https://onlinelibrary.wiley.com/doi/10.1002/anie.202507332 by Tianjin University Of, Wiley Online Library on [0610/2025]. See the Terms and Conditions (https://onlinelibrary.wiley.com/emrs-and-conditions) on Wiley Online Library for rules of use; OA arctices are governed by the applicable Creative Commons Licensea

15213773, 2025, 29, Downloaded from https://onlinelibrary.wiley.com/oi/10.1002/anie.202507332 by Tanjan University Of, Wiley Online Library on 106/10/2025, See the Terms and Conditions (https://onlinelibrary.wiley.com/terms-and-conditions) on Wiley Online Library for rules of use; OA articles are governed by the applicable Creative Commons License

corresponding to the binding energies of pyridine-N and N—C=O, respectively. Upon light illumination, the signal of pyridine-N shifts to 399.2 eV (Figure S30). [41.69] Moreover, the signals of both C 1 s and O 1 s keep unchanged upon light illumination compared with those in the dark (Figure S31). These results imply that the photogenerated electrons in HOF-8 transfer to Pt to reduce  $H^+$  to  $H_2$ .

#### Conclusion

In summary, two HOFs (HOF- $8^{[42]}$  and HOF-TUT-8) with similar 3D structures were successfully constructed, which can be used as heterogeneous photocatalysts for  $H_2$  evolution. HOF-8 possesses abundant  $\pi$ - $\pi$  stacking interactions, exhibiting more efficient charge separation and transfer than HOF-TUT-8 without  $\pi$ - $\pi$  stacking. As a result, HOF-8 achieves a higher  $H_2$  production rate of 1914.4  $\mu$ mol  $g^{-1}$  h<sup>-1</sup>, which is 3.3 times higher than that of HOF-TUT-8. Systematic studies demonstrate that the  $\pi$ - $\pi$  stacking in HOF-8 can serve as an electron-transfer channel to fast transfer electrons to achieve high-efficiency photocatalytic  $H_2$  evolution. This study directly evidences the intrinsic role of  $\pi$ - $\pi$  stacking as electron transfer-channels in photocatalysis and highlights an efficient way to enhance photocatalytic activity for  $H_2$  evolution.

### Acknowledgements

This work was supported by the National Natural Science Foundation of China (22271218), the Natural Science Foundation of Tianjin City (24JCZDJC00220), and the National Key R&D Program of China (2022YFA1502902).

#### **Conflict of Interests**

The authors declare no conflict of interest.

#### **Data Availability Statement**

The data that support the findings of this study are available in the supplementary material of this article.

**Keywords:**  $H_2$  evolution • Hydrogen-bonded organic frameworks • Photocatalysis •  $\pi$  frameworks •  $\pi$ – $\pi$  stacking interaction

- D. Voiry, H. S. Shin, K. P. Loh, M. Chhowalla, *Nat. Rev. Chem.* 2018, 2, 0105.
- [2] D.-C. Zhong, Y.-N. Gong, C. Zhang, T.-B. LuChem. Soc. Rev. 2023, 52, 3170–3214.
- [3] J. Li, H. Huang, W. Xue, K. Sun, X. Song, C. Wu, L. Nie, Y. Li, C. Liu, Y. Pan, H.-L. Jiang, D. Mei, C. Zhong, *Nat. Catal.* 2021, 4, 719–729.

- [4] Z. Jiang, X. Xu, Y. Ma, H. S. Cho, D. Ding, C. Wang, J. Wu, P. Oleynikov, M. Jia, J. Cheng, Y. Zhou, O. Terasaki, T. Peng, L. Zan, H. Deng, *Nature* 2020, 586, 549–554.
- [5] D.-C. Liu, D.-C. Zhong, T.-B. Lu, EnergyChem 2020, 2, 100034.
- [6] M. Zhang, M. Lu, Z.-L. Lang, J. Liu, M. Liu, J.-N. Chang, L.-Y. Li, L.-J. Shang, M. Wang, S.-L. Li, Y.-Q. Lan, Angew. Chem. Int. Ed. 2020, 132, 6500–6506; Angew. Chem. 2020, 132, 6562–6568.
- [7] Y. Li, J.-F. Sui, L.-S. Cui, H.-L. Jiang, J. Am. Chem. Soc. 2023, 145, 1359–1366.
- [8] J. Li, J. Zhou, X.-H. Wang, C. Guo, R.-H. Li, H. Zhuang, W. Feng, Y. Hua, Y.-Q. Lan, *Angew. Chem. Int. Ed.* 2024, e202411721.
- [9] A.-A. Zhang, Z.-X. Wang, Z.-B. Fang, J.-L. Li, T.-F. Liu, Angew. Chem. Int. Ed. 2024, 63, e202412777.
- [10] C. Zhu, C. Gong, D. Cao, L.-L. Ma, D. Liu, L. Zhang, Y. Li, Y. Peng, G. Yuan, *Angew. Chem. Int. Ed.* 2025, 64, e202504348.
- [11] Y.-N. Gong, J.-H. Mei, W.-J. Shi, J.-W. Liu, D.-C. Zhong, T.-B. Lu, Angew. Chem. Int. Ed. 2024, 63, e202318735.
- [12] J.-W. Wang, L.-Z. Qiao, H.-D. Nie, H.-H. Huang, Y. Li, S. Yao, M. Liu, Z.-M. Zhang, Z.-H. Kang, T.-B. Lu, *Nat. Commun.* 2021, 12, 813.
- [13] J.-W. Wang, M. Gil-Sepulcre, H.-H. Huang, E. Solano, Y.-F. Mu, A. Llobet, G. Ouyang, Cell Rep. Phys. Sci. 2021, 2, 100681.
- [14] W. Yang, R. Godin, H. Kasap, B. Moss, Y. Dong, S.-A.-J. Hillman, L. Steier, E. Reisner, J.-R. Durrant, J. Am. Chem. Soc. 2019, 141, 11219–11229.
- [15] A. Nakada, K. Koike, T. Nakashima, T. Morimoto, O. Ishitani, *Inorg. Chem.* 2015, 54, 1800–1807.
- [16] A. Nakada, K. Koike, K. Maeda, O. Ishitani, Green. Chem. 2016, 18, 139–143.
- [17] Y. Yamazaki, O. Ishitani, Chem. Sci. 2018, 9, 1031–1041.
- [18] A.-M. Cancelliere, F. Puntoriero, S. Serroni, S. Campagna, Y. Tamaki, D. Saito, O. Ishitani, Chem. Sci. 2020, 11, 1556–1563.
- [19] D.-C. Fabry, H. Koizumi, D. Ghosh, Y. Yamazaki, H. Takeda, Y. Tamaki, O. Ishitani, Organometallics 2020, 39, 1511–1518.
- [20] Y. Kuramochi, Y. Fujisawa, A. Satake, J. Am. Chem. Soc. 2020, 142, 705–709.
- [21] J.-W. Wang, L. Jiang, H.-H. Huang, Z. Han, G. Ouyang, *Nat. Commun.* 2021, 12, 4276.
- [22] B. Ma, G. Chen, C. Fave, L. Chen, R. Kuriki, K. Maeda, O. Ishitani, T.-C. Lau, J. Bonin, M. Robert, J. Am. Chem. Soc. 2020, 142, 6188–6195.
- [23] Y. Wei, L. Chen, H. Chen, L. Cai, G. Tan, Y. Qiu, Q. Xiang, G. Chen, T.-C. Lau, M. Robert, *Angew. Chem. Int. Ed.* 2022, 61, e202116832; *Angew. Chem.* 2022, 134, e202116832.
- [24] G. Zhao, H. Pang, G. Liu, P. Li, H. Liu, H. Zhang, L. Shi, J. Ye, Appl. Catal. B Environ. Energy 2017, 200, 141–149.
- [25] L. Lin, C. Hou, X. Zhang, Y. Wang, Y. Chen, T. He, *Appl. Catal. B Environ. Energy* 2018, 221, 312–319.
- [26] P.-L. Cheung, S.-C. Kapper, T. Zeng, M.-E. Thompson, C.-P. Kubiak, J. Am. Chem. Soc. 2019, 141, 14961–14965.
- [27] J.-W. Wang, Z. Li, Z.-M. Luo, Y. Huang, F. Ma, S. Kupfer, G. Ouyang, Proc. Natl. Acad. Sci. U.S.A. 2023, 120, e2221219120.
- [28] J.-W. Wang, H.-H. Huang, P. Wang, G. Yang, S. Kupfer, Y. Huang, Z. Li, Z. Ke, G. Ouyang, JACS Au 2022, 2, 1359–1374
- [29] H. Nasrallah, P. Lyu, G. Maurin, M. El-Roz, J. Catal. 2021, 404, 46–55.
- [30] L.-Q. Qiu, K.-H. Chen, Z.-W. Yang, L.-N. He, Green. Chem. 2020, 22, 8614–8622.
- [31] Y. He, S. Xiang, B. Chen, J. Am. Chem. Soc. **2011**, 133, 14570–
- [32] Y. Li, X. Wang, H. Zhang, L. He, J. Huang, W. Wei, Z. Yuan, Z. Xiong, H. Chen, S. Xiang, B. Chen, Z. Zhang, *Angew. Chem. Int. Ed.* 2023, 62, e202311419.
- [33] Q. Yin, E.-V. Alexandrov, D.-H. Si, Q.-Q. Huang, Z.-B. Fang, Y. Zhang, A.-A. Zhang, W.-K. Qin, Y.-L. Li, T.-F. Liu, D.-M.

15213773, 2025, 29, Downloaded from https://onlinelibrary.wiley.com/doi/10.1002/mie.202507332 by Tianjin University Of, Wiley Online Library on [06/10/2025]. See the Terms and Conditions (https://onlinelibrary.wiley.com/terms/

and-conditions) on Wiley Online Library for rules of

use; OA articles are governed by the applicable Creative Commons License

## Research Article



- Proserpio, Angew. Chem. Int. Ed. 2022, 61, e202115854; Angew. Chem. 2022, 134, e202115854.
- [34] N. Zhang, Q. Yin, S. Guo, K.-K. Chen, T.-F. Liu, P. Wang, Z.-M. Zhang, T.-B. Lu, Appl. Catal. B Environ. Energy 2021, 296, 120337.
- [35] X. Gao, W. Lu, Y. Wang, X. Song, C. Wang, K.-O. Kirlikovali, P. Li, Sci. China Chem. 2022, 65, 2077–2095.
- [36] Q. Zhou, Y. Guo, Y. Zhu, Nat. Catal. 2023, 6, 574–584.
- [37] B. Yu, L. Li, S. Liu, H. Wang, H. Liu, C. Lin, C. Liu, H. Wu, W. Zhou, X. Li, T. Wang, B. Chen, J. Jiang, *Angew. Chem. Int. Ed.* 2021, 133, 8983–8989; *Angew. Chem.* 2021, 133, 9065–9071.
- [38] S. Huang, Y. Chang, Z. Li, J. Cao, Y. Song, J. Gao, L. Sun, J. Hou, Adv. Funct. Mater. 2023, 33, 2211631.
- [39] X.-T. He, Y.-H. Luo, Z.-Y. Zheng, C. Wang, J.-Y. Wang, D.-L. Hong, L.-H. Zhai, L.-H. Guo, B.-W. Sun, ACS Appl. Nano Mater 2019, 2, 7719–7727.
- [40] A.-A. Zhang, D. Si, H. Huang, L. Xie, Z.-B. Fang, T.-F. Liu, R. Cao, Angew. Chem. Int. Ed. 2022, 61, e202203955; Angew. Chem. 2022, 134, e202203955.
- [41] C.-J. Lu, W.-J. Shi, Y.-N. Gong, J.-H. Zhang, Y.-C. Wang, J.-H. Mei, Z.-M. Ge, T.-B. Lu, D.-C. Zhong, *Angew. Chem. Int. Ed.* 2024, 63, e202405451.
- [42] X.-Z. Luo, X.-J. Jia, J.-H. Deng, J.-L. Zhong, H.-J. Liu, K.-J. Wang, D.-C. Zhong, J. Am. Chem. Soc. 2013, 135, 11684–11687.
- [43] W.-J. Liu, Y.-Q. Wen, J.-W. Wang, D.-C. Zhong, J.-B. Tan, T.-B. Lu, J. Mater. Chem. A 2019, 7, 9587–9592.
- [44] Y. Sang, Q. Zhu, X. Zhou, Y. Jiang, L. Zhang, M. Liu, Angew. Chem. Int. Ed. 2023, 62, e202215867; Angew. Chem. 2023, 135, e202215867.
- [45] Y. Bi, Z. Wang, T. Liu, D. Sun, N. Godbert, H. Li, J. Hao, X. Xin, ACS Nano 2021, 15, 15910–15919.
- [46] M. Xue, Y. Lü, Q. Sun, K. Liu, Z. Liu, P. Sun, Cryst. Growth Des 2015, 15, 5360–5367.
- [47] S. Sengupta, A. Goswami, R. Mondal, New J. Chem. 2014, 38, 2470.
- [48] Z. Džolić, M. Cametti, D. Milić, M. Žinić, Chem. Eur. J. 2013, 19, 5411–5416.
- [49] S. Mohata, R. Das, K. Koner, M. Riyaz, K. Das, S. Chakraborty, Y. Ogaeri, Y. Nishiyama, S.-C. Peter, R. Banerjee, J. Am. Chem. Soc. 2023, 145, 23802–23813.
- [50] P. Das, G. Chakraborty, J. Roeser, S. Vogl, J. Rabeah, A. Thomas, J. Am. Chem. Soc. 2023, 145, 2975–2984.
- [51] Y. Liu, Y. Wang, J. Shang, J. Peng, T. Zhu, Appl. Catal. B Environ. Energy 2024, 350, 123937.
- [52] R. Sun, X. Hu, C. Shu, L. Zheng, S. Wang, X. Wang, B. Tan, Chin. J. Catal. 2023, 55, 159–170.

- [53] Q. Li, J.-N. Chang, Z. Wang, M. Lu, C. Guo, M. Zhang, T.-Y. Yu, Y. Chen, S.-L. Li, Y.-Q. Lan, J. Am. Chem. Soc. 2023, 145, 23167–23175.
- [54] C. Chen, Z. Di, H. Li, J. Liu, M. Wu, M. Hong, CCS Chem 2022, 4, 1315–1325.
- [55] Y. Zhang, C. Pan, G. Bian, J. Xu, Y. Dong, Y. Zhang, Y. Lou, W. Liu, Y. Zhu, Nat. Energy 2023, 8, 361–371.
- [56] D. Chu, W. Gong, H. Jiang, X. Tang, Y. Cui, Y. Liu, CCS Chem 2022, 4, 1180–1189.
- [57] L. An, P.-D.-L. Torre, P.-T. Smith, M.-R. Narouz, C.-J. Chang, Angew. Chem. Int. Ed. 2023, 62, e202209396; Angew. Chem. 2023, 135, e202209396.
- [58] Y. Pellegrin, F. Odobel, C. R. Chim. 2017, 20, 283–295.
- [59] H. Wang, X. Zhang, W. Zhang, M. Zhou, H.-L. Jiang, Angew. Chem. Int. Ed. 2024, 63, e202401443.
- [60] N.-Y. Huang, J.-Q. Shen, X.-W. Zhang, P.-Q. Liao, J.-P. Zhang, X.-M. Chen, J. Am. Chem. Soc. 2022, 144, 8676–8682.
- [61] J.-H. Zhang, Y.-N. Gong, H.-J. Wang, Y.-C. Wang, W. Yang, J.-H. Mei, D.-C. Zhong, T.-B. Lu, Proc. Natl. Acad. Sci. U.S.A. 2022, 119, e2118278119.
- [62] Y.-N. Gong, J.-H. Mei, J.-W. Liu, H.-H. Huang, J.-H. Zhang, X. Li, D.-C. Zhong, T.-B. Lu, Appl. Catal. B Environ. Energy 2021, 292, 120156.
- [63] D. Cong, J. Sun, Y. Pan, X. Fang, L. Yang, W. Zhou, T. Yu, Z. Li, C. Liu, W.-Q. Deng, *Angew. Chem. Int. Ed.* 2024, 63, e202316991.
- [64] C. Li, H. Xu, H. Xiong, S. Xia, X. Peng, F. Xu, X. Chen, Adv. Funct. Mater. 2024, 34, 2405539.
- [65] S.-F. Chen, Y.-F. Hu, L. Ji, X.-L. Jiang, X.-L. Fu, Appl. Surf. Sci. 2014, 292, 357–366.
- [66] N. Tian, H.-W. Huang, Y. He, Y.-X. Guo, T.-R. Zhang, Y.-H. Zhang, *Dalton Trans.* 2015, 44, 4297–4307.
- [67] Y. Yang, X. Chu, H.-Y. Zhang, R. Zhang, Y.-H. Liu, F.-M. Zhang, M. Lu, Z.-D. Yang, Y.-Q. Lan, Nat. Commun. 2022, 14, 593
- [68] N. Liu, J. Jiang, Z. Chen, B. Wu, S. Zhang, Y.-Q. Zhang, P. Cheng, W. Shi, Angew. Chem. Int. Ed. 2023, 62, e202312306; Angew. Chem. 2023, 135, e202312306.
- [69] J. Zhou, J. Li, L. Kan, L. Zhang, Q. Huang, Y. Yan, Y. Chen, J. Liu, S.-L. Li, Y.-Q. Lan, Nat. Commun. 2022, 13, 4681.

Manuscript received: April 01, 2025 Revised manuscript received: May 10, 2025 Accepted manuscript online: May 13, 2025 Version of record online: May 20, 2025